ROOM
-VENT
'90

Convection from a slender cylinder in a ventilated room

Per Heiselberg
University of Aalborg
Aalborg, Denmark

Mats Sandberg
The National Swedish Institute for Building Research
Gävle, Sweden

B2

Session B 2 – 4

34

CONVECTION FROM A SLENDER CYLINDER IN A VENTILATED ROOM

Per Heiselberg
University of Aalborg
Aalborg, Denmark

Mats Sandberg
The National Swedish Institute for
Building Research
Gävle, Sweden

SUMMARY

The equations, based on an integral formulation, for turbulent natural boundary layer flow are solved in both the constant temperature case and in the constant heat flux case. Solutions are found for convection along both flat plates and cylinders. Theoretical predictions are compared with measurements in the boundary layer flow around a heated vertical slender cylinder in a full-scale test room with displacement ventilation. Both velocity and temperature profiles in the boundary layer flow were recorded.

The room was ventilated by a low velocity diffuser, standing on the floor, from which air with a negative buoyancy was supplied. The vertical distribution of both temperature and contamination in the room was measured as a function of the heat load and the air flow rate. The contaminant distribution showed a clear stratification between clean and contaminated air, while the temperature was increasing uniformly from floor to ceiling. It was found that the convective flow at the heat source as well as the flow at the walls was influencing the level of stratification.

NOMENCLATURE

A	Constant	
B	Constant	
C	Constant	
c	Concentration	(ppm)
c_{max}	Maximum concentration in room	(ppm)
c_p	Specific heat at constant pressure	(J/kg^oC)
D	Cylinder diameter	(m)
E	Power supply, Energy flow	(W)
g	Acceleration of gravity	(m/s^2)
H	Room height	(m)
k	Thermal conductivity	(W/m^oC)
L	Room lenght	(m)
m	Power low constant	
n	Power low constant, specific air flow rate	(roomv./h)

p	Power low constant	
q_b	Boundary layer flow	$(m^3/s \cdot m)$
q''	Surface heat flux	(W/m^2)
q_v	Volumetric flow rate	(m^3/s)
r_o	Cylinder radius	(m)
t	Temperature in boundary layer	(^oC)
t_∞	Ambient temperature	(^oC)
t_w	Surface temperature	(^oC)
ΔT	Temperature difference $(t-t_\infty)$	(^oC)
ΔT_w	Surface temperature difference (t_w-t_∞)	(^oC)
t_{par}	Parameter temperature $t_{par} = 1/2(t_\infty+t_w)$	(^oC)
T	Room temperature	(^oC)
T_A	Ambient temperature	(^oC)
T_S	Supply air temperature	(^oC)
T_E	Exhaust air temperature	(^oC)
T_w	Wall temperature	(^oC)
U	Mean velocity component in x-direction	(m/s)
U_1	Characteristic velocity	(m/s)
U_x	Maximum mean velocity in boundary layer	(m/s)
$\dot{V}$	Volume flow in boundary layer	(m^3/s)
W	Room width	(m)
x	Distance upstream from leading edge	(m)
y	Distance normal to plate surface	(m)
β	Coefficient of thermal expansion	(/k)
δ	Boundary layer thickness	(m)
δ_h	Thermal displacement thickness	(m)
δ^*	Displacement thickness	(m)
ρ	Air density	(kg/m^3)
τ_w	Wall shearing stress	(N/m^2)
ν	Kinematic viscosity	(m^2/s)
Pr	Prandtl number, $Pr = \frac{\rho c_p \nu}{k}$	
Gr_x	Grashof number, $Gr_x = \frac{g\beta\Delta T_w x^3}{\nu^2}$	
Gr_x^*	Modified Grashof number, $Gr_x^* = \frac{g\beta q'' x^4}{k\nu^2}$	

INTRODUCTION

Natural convection in enclosures is a topic of great engineering interest due to the many applications that occur in various fields. Within ventilation engineering it has become an important topic due to the introduction of displacement ventilation. For design of this type of ventilation it is necessary to know the flow rates created by different heat sources in the room. However, most studies, both theoretical and experimental, have been focused on entirely closed enclosures with a flow in the laminar regime. Neither of these two conditions is fulfilled in a ventilated room. Furthermore, most measurements of turbulent natural convection boundary layer are from plates with constant wall temperatures. However, the temperatures of the walls encountered in buildings float such that the temperature with altitude increases. Therefore, a more appropriate model case for buildings seems to be the constant heat flux case.

In this paper the equations, based on integral formulation, for the boundary layer flow in the constant heat flux case and in the constant temperature case have been solved, and both a flat plate and a cylinder solution are presented. Results are compared with measurements carried out in the turbulent boundary layer flow along a slender cylinder. An additional complication that arises in air is that air is transparent to long wave thermal radiation. This will influence the temperature field in the room. The vertical distribution of both room temperature, wall temperature and contamination are recorded and the results are discussed.

TEST ROOM AND EXPERIMENTAL APPARATUS

The tests were performed at the Swedish Institute for Building Research in a mock-up of a common type of office room. Its dimensions were 4.2 m × 3.6 m × 2.5 m (L × W × H). This gives a room volume of 38 m^3, see figure 1.

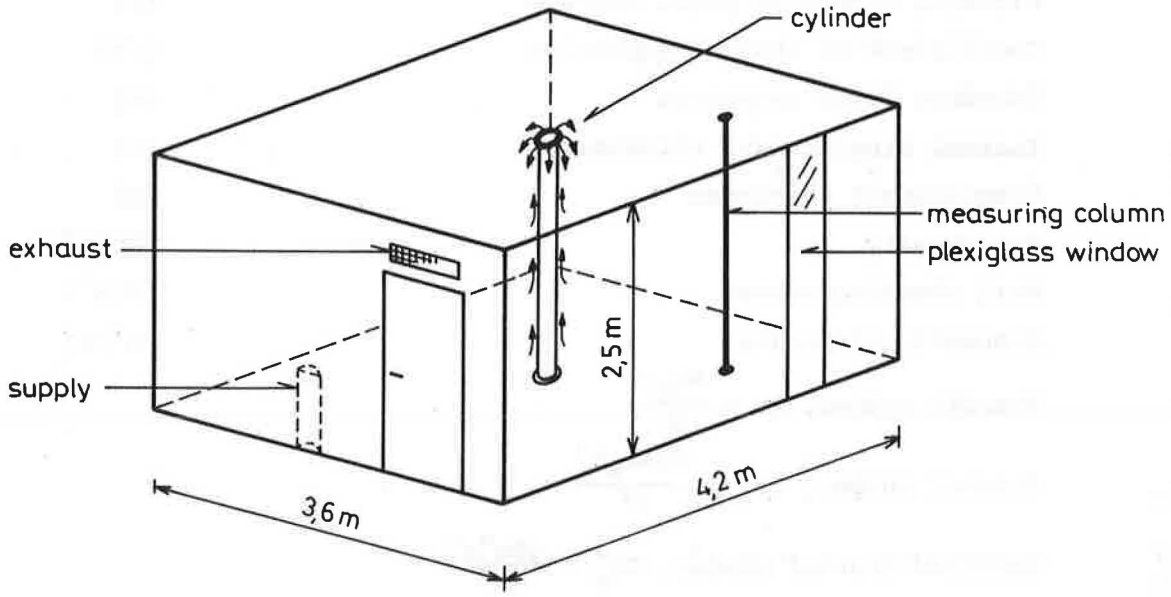

Figure 1. Test room with a low velocity diffuser and a slender cylinder in the middle.

In all tests air with a negative buoyancy was supplied through a low velocity diffuser standing on the floor at the rear wall. The air left the room through a grille at the ceiling. A cylinder (diameter 0.1 m) in the form of a pillar from floor to ceiling was placed in the middle of the room. The cylinder was heated by resistance heating along its whole height. The heat loss from the cylinder, due to convection, amounted to about 89% of the total heat output.

The following temperatures were recorded in the tests:

Cylinder surface temperature (12 points).

Wall surface temperature (4 × 6 points).

Ceiling and floor surface temperature.

Room air temperature (24 points).

Temperature in adjacent room.

Temperatures in the boundary layer along the cylinder (10 points).

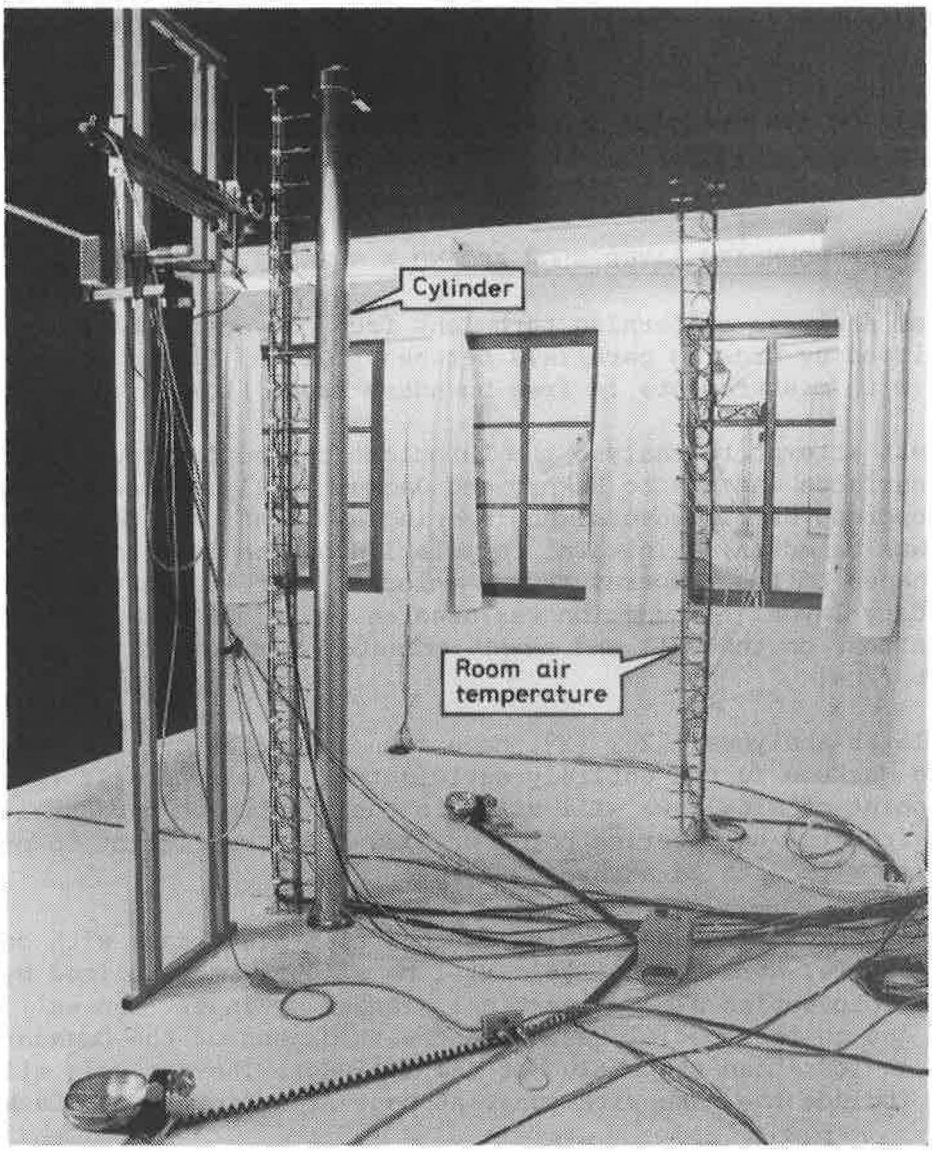

Temperatures in the boundary layer flow around the cylinder were recorded with 10 thermocouples located from 0.5 - 1 mm from the cylinder surface up to 250 mm distance from the surface. They were recorded at four heights above the floor, 0.2 m, 0.8 m, 1.4 m and 2.0 m, respectively. The temperatures in the boundary layer have been corrected for the influence of radiation from the cylinder.

The temperatures were recorded at several combinations of ventilation air flow rate, q_v, and power supply, E, to the cylinder.

The velocities in the boundary layer flow were recorded with a hot wire anemometer with temperature compensation. They were recorded at 10 different heights above the floor, at some heights twice. The location of the anemometer was controlled by a motor driven traversing mechanism that was hand operated. In each height the velocities were measured in 10 - 20 different distances from 1 mm to 500 mm from the cylinder surface. The velocities were recorded only for one combination of air flow rate (q_v = 0.053 m^3/s) and power supply to the cylinder (E = 600 W).

The vertical distribution of contamination was found by measuring the concentration of tracer gas in 10 heights above the floor. The tracer gas was released in three different locations in the room. It was released into the boundary layer flow around the cylinder, into the room outside the boundary layer flow, above and below the level of stratification, respectively. Total power supply to the cylinder amounted to 600 W which corresponds to a surface heat flux of 764 W/m^2.

BOUNDARY LAYER FLOW AROUND A SLENDER CYLINDER

Theoretical analyses concerning turbulent free convection boundary layers have developed by drawing parallels between free and forced convection complemented with measurements in free boundary layer flows.

The earliest attempt to analyse the turbulent convection boundary layer on vertical surfaces was due to Eckert and Jackson, [11], whose approach has found widespread use in several engineering applications. Eckert and Jackson's approach was based on an integral formulation of the problem. They assumed certain shapes of the temperature and velocity profiles in the free convection boundary layer. In addition was used an empirical relation for the shearing stress on the wall and a heat transfer coefficient derived from forced convective flow.

Although later analyses, [2], [3], have found that the original approach by Eckert and Jackson is not entirely satisfactory in all details (from the theoretical point of view), we will stick to their approach because it is widely used, and from the engineering point of view it is sufficient to predict the correct flow rate with an accuracy of 10%.

Eckert and Jackson found a solution for the flat plate case with constant surface temperature. Here the analysis will be slightly generalized by studying the natural convection along a vertical slender cylinder. The wall case will then come out as the special case when the thickness of the boundary layer flow is much less than the radius of the cylinder. The analysis will be extended to include the case with constant heat flux from the surface.

Theory for Turbulent Natural Convection Flows

Equations for momentum and heat flow are sufficient to calculate the boundary layer thickness and the maximum velocity when the shape of the temperature and velocity profiles within the boundary layer and the laws for the shearing stress and the heat flow on the wall are known.

With the notation in figure 2 the equations for momentum and heat flow will be

$$\frac{d}{dx}\int_{r_o}^{r_o+\delta} U^2\, 2\pi r dr = g\beta \int_{r_o}^{r_o+\delta} \Delta T\, 2\pi r dr - \frac{\tau_w r_o}{\rho} \tag{1}$$

$$\rho c_p \frac{d}{dx}\int_{r_o}^{r_o+\delta} \Delta T\, U\, 2\pi r dr = q'' 2\pi r_o - \rho c_p q_b 2\pi r_o \frac{dt_\infty}{dx} \tag{2}$$

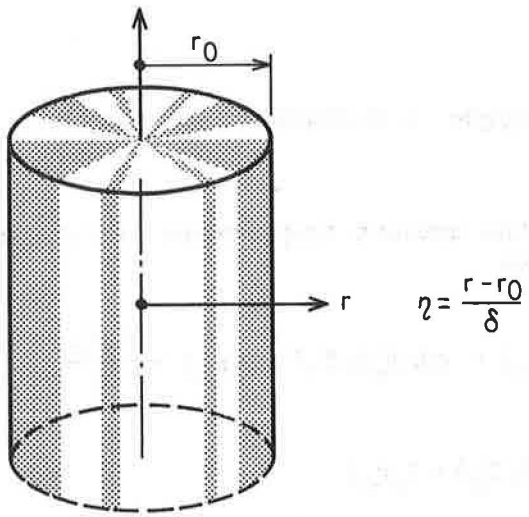

Figure 2. Notation

Eckert and Jackson, [1], analysed measurements by Griffiths and Davis, [4], and they approximated the recorded temperature and velocity profiles with the following relations.

$$\Delta T(x,\eta) = \Delta T_w(x) f_T(\eta) = \Delta T_w(x)(1-\eta^{1/7}) \tag{3}$$

$$U(x,\eta) = U_1(x) f_v(\eta) = U_1(x)(\eta^{1/7}(1-\eta)^4) \tag{4}$$

By introducing the following integrals

$$I_1 = \int_o^1 f_v(\eta) d\eta \qquad = 0.146 \tag{5}$$

$$I_2 = \int_o^1 f_v(\eta)^2 d\eta \qquad = 0.0523 \tag{6}$$

$$I_3 = \int_o^1 f_t(\eta)d\eta \qquad = 0.125 \tag{7}$$

$$I_4 = \int_o^1 f_v(\eta)f_t(\eta)d\eta \quad = 0.0366 \tag{8}$$

$$I_5 = \int_o^1 f_v(\eta)\eta d\eta \qquad = 0.0272 \tag{9}$$

$$I_6 = \int_o^1 f_v(\eta)^2\eta d\eta \qquad = 0.00654 \tag{10}$$

$$I_7 = \int_o^1 f_t(\eta)\eta d\eta \qquad = 0.0333 \tag{11}$$

$$I_8 = \int_o^1 f_v(\eta)f_t(\eta)\eta d\eta \quad = 0.00479 \tag{12}$$

and by assuming that the ambient temperature is constant the equations (1) and (2) can be rewritten as

$$\frac{d}{dx}\,(U_1^2\delta(I_6\delta + I_2 r_o) = g\beta\Delta T_w\delta(I_7\delta + I_3 r_o) - \frac{\tau_w r_o}{\rho} \tag{13}$$

$$\frac{q'' r_o}{\rho c_p} = \frac{d}{dx}\,(U_1\Delta T_w\delta(I_8\delta + I_4 r_o) \tag{14}$$

At this stage we have two equations for four unknowns (U_1, δ, ΔT_w, q''). In order to solve the problem Eckert and Jackson made two additional assumptions.

The wall shear stress τ_w depends on the velocity scale U_1 in the same manner as in forced convection.

$$\tau_w = 0.0225\ \rho U_1^2 (\frac{\nu}{U_1\delta})^{1/4} \tag{15}$$

The local shear stress and the heat flux are related through the relationship

$$\frac{q''}{\rho c_p U_1 \Delta T_w}\,Pr^{2/3} = \frac{\tau_w}{\rho U_1^2} \tag{16}$$

The flat plate case (δ<<D) can be solved by assuming power law expressions for the velocity, the temperature difference and the boundary layer thickness.

$$U_1 = Ax^m \quad ; \quad \delta = Bx^n \quad ; \quad \Delta T_w = Cx^P \tag{17}$$

The equations for the flat plate case are optained by setting the integrals I_5 to I_8 equal to zero.

The solution for constant surface temperature becomes

$$U_1 = 1.186 \frac{\nu}{x} Gr_x^{1/2} [1 + 0.494 \ Pr^{2/3}]^{-1/2} \tag{18}$$

$$\delta = 0.566 \ xGr_x^{-1/10} Pr^{-8/15} [1 + 0.494 \ Pr^{2/3}]^{1/10} \tag{19}$$

The solution for constant heat flux from the surface becomes

$$U_1 = 4.35 \frac{\nu}{x} Gr_x^{*5/14} Pr^{-1/6} [1 + 0.445 \ Pr^{2/3}]^{-5/14} \tag{20}$$

$$\delta = 0.505 \ xGr_x^{*-1/14} Pr^{-1/2} [1 + 0.445 \ Pr^{2/3}]^{1/14} \tag{21}$$

$$\Delta T_w = 12.44 \left(\frac{\nu^2}{g\beta}\right) \frac{1}{x^3} (Gr_x^*)^{5/7} Pr^{-1/3} [1 + 0.445 \ Pr^{2/3}]^{2/7} \tag{22}$$

It is possible to simplify the equations (18) - (22) by inserting the material constants. In figure 3 simplified expressions for air are shown with material constants inserted at the temperatur t_{par} = 20°C. Expressions for volume and energy flow in the boundary layer are also shown.

The maximum velocity, U_x, in the boundary layer is used instead of the velocity scale U_1. U_x is found by differentiating equation (4).

Constant surface temperature, ΔT_w			
$U_x = 0.099$	$\Delta T_w^{1/2}$	$x^{1/2}$	(m/s)
$\delta = 0.107$	$\Delta T_w^{-1/10}$	$x^{7/10}$	(m)
$\dot{V} = 2.88 \cdot 10^{-3}$	$\Delta T_w^{2/5}$	$x^{6/5}$	(m^3/s)
$E = 0.875$	$\Delta T_w^{7/5}$	$x^{6/5}$	(W)
Constant heat flux from the surface, q"			
$U_x = 0.102$	$q''^{5/14}$	$x^{3/7}$	(m/s)
$\delta = 0.123$	$q''^{-1/14}$	$x^{5/7}$	(m)
$\Delta T_w = 0.963$	$q''^{5/7}$	$x^{-1/7}$	(°C)
$\dot{V} = 3.41 \cdot 10^{-3}$	$q^{2/7}$	$x^{8/7}$	(m^3/s)
$E =$	q''	x	(W)

Figure 3. Simplified expressions for the solution in the flat plate case t_{par} = 20°C.

It is not possible to find an exact solution for the turbulent natural convection boundary layer flow around a cylindrical surface. The solution is therefore found numerically using a standard Runga-Kutta routine. The relations in figure 4 are a result of the best fit of the numerical solutions and they also apply to $t_{par} = 20^{o}C$.

Constant surface temperature, ΔT_w					
$U_x = 0.099$		$\Delta T_w^{1/2}$	$x^{1/2}$	$(1-e^{-4.9\, r_o})^{-0.057}$	(m/s)
$\delta = 0.107$		$\Delta T_w^{-1/10}$	$x^{7/10}$	$(1-e^{-12.0\, r_o})^{0.30}$	(m)
$\dot{V} = 2.88 \cdot 10^{-3}$	$2\pi r_o$	$\Delta T_w^{2/5}$	$x^{6/5}$	$(1-e^{-8.1\, r_o})^{-0.17}$	(m^3/s)
$E = 0.875$	$2\pi r_o$	$\Delta T_w^{7/5}$	$x^{6/5}$	$(1-e^{-13.3\, r_o})^{-0.12}$	(W)
Constant heat flux from the surface, q"					
$U_x = 0.102$		$q''^{5/14}$	$x^{3/7}$	$(1-e^{-2.7\, r_o})^{-0.025}$	(m/s)
$\delta = 0.123$		$q''^{-1/14}$	$x^{5/7}$	$(1-e^{-12.2\, r_o})^{0.30}$	(m)
$\Delta T_x = 0.963$		$q''^{5/7}$	$x^{-1/7}$	$(1-e^{-7.1\, r_o})^{0.086}$	(^{o}C)
$\dot{V} = 3.41 \cdot 10^{-3}$	$2\pi r_o$	$q''^{2/7}$	$x^{8/7}$	$(1-e^{-6.8\, r_o})^{-0.16}$	(m^3/s)
$E =$	$2\pi r_o$	q"	x		(W)

Figure 4. Simplified expressions for the solution in the cylinder case $t_{par} = 20^{o}C$.

The expressions in the figures 3 and 4 show that the maximum velocity is greater and that the boundary layer thickness is smaller for turbulent free convection flow around a cylinder that along a flat plate.

Comparison with Measurements

The numerical solution is compared with measurements in the natural convection boundary layer along a slender cylinder with constant heat flux from the surface placed in a full-scale test room.

In the figures 5 and 6 the recorded profiles of temperature and velocity are shown together with the assumed profiles by Eckert and Jackson.

The temperature in figure 5 is normalized by the temperature difference between the cylinder surface and the ambient room air temperature. The boundary layer thickness, δ, was arbitrarily defined by Eckert and Jackson such that the distance where $\Delta T/\Delta T_w$ had the value 0.2 was set equal to 0.5. In order to be able to compare the measurements with the assumed profile by Eckert and Jackson the data were normalized by the thermal (enthalpy) displacement thickness defined as:

$$\delta_h = \int_0^\infty \frac{\Delta T}{\Delta T_w} \, dy \tag{23}$$

If the thermal displacement thickness is inserted in equation (3) it becomes:

$$\frac{\Delta T}{\Delta T_w} = 1 - \left(\frac{y}{8\delta_h}\right)^{1/7} \tag{24}$$

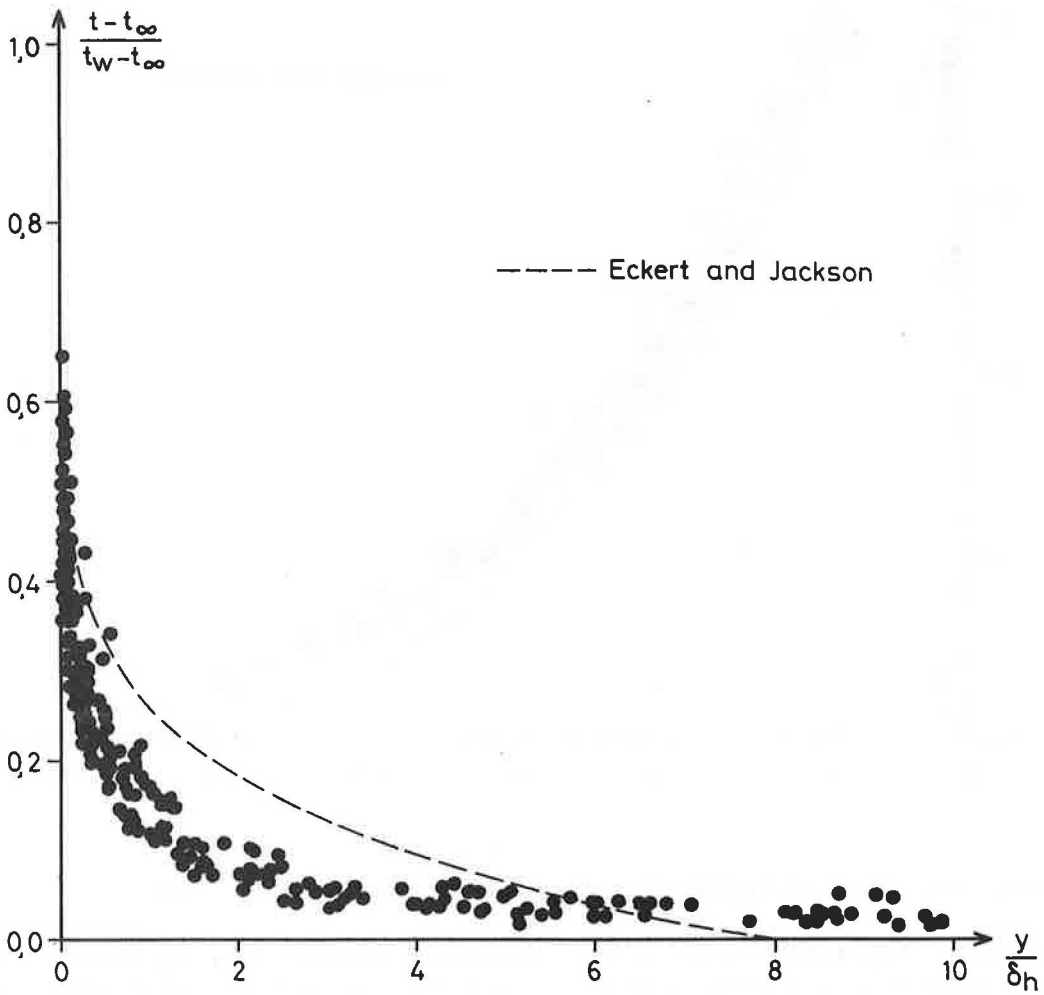

Figure 5. Recorded temperature distribution in the boundary layer.

The velocities in figure 6 are normalized by the maximum recorded velocity. Eckert and Jackson normalized their data such that U/U_x had the value 0.5 at a distance equal to 1. Here the data are normalized by use of the displacement thickness, δ^*, defined as:

$$\delta^* = \int_0^\infty \frac{U}{U_x} \, dy \tag{25}$$

If the displacement thickness is inserted in equation (4) it becomes:

$$\frac{U}{U_x} = 1{,}86\left(\frac{y}{3.7\delta^*}\right)^{1/7}\left(1 - \frac{y}{3.7\delta^*}\right)^4 \qquad (26)$$

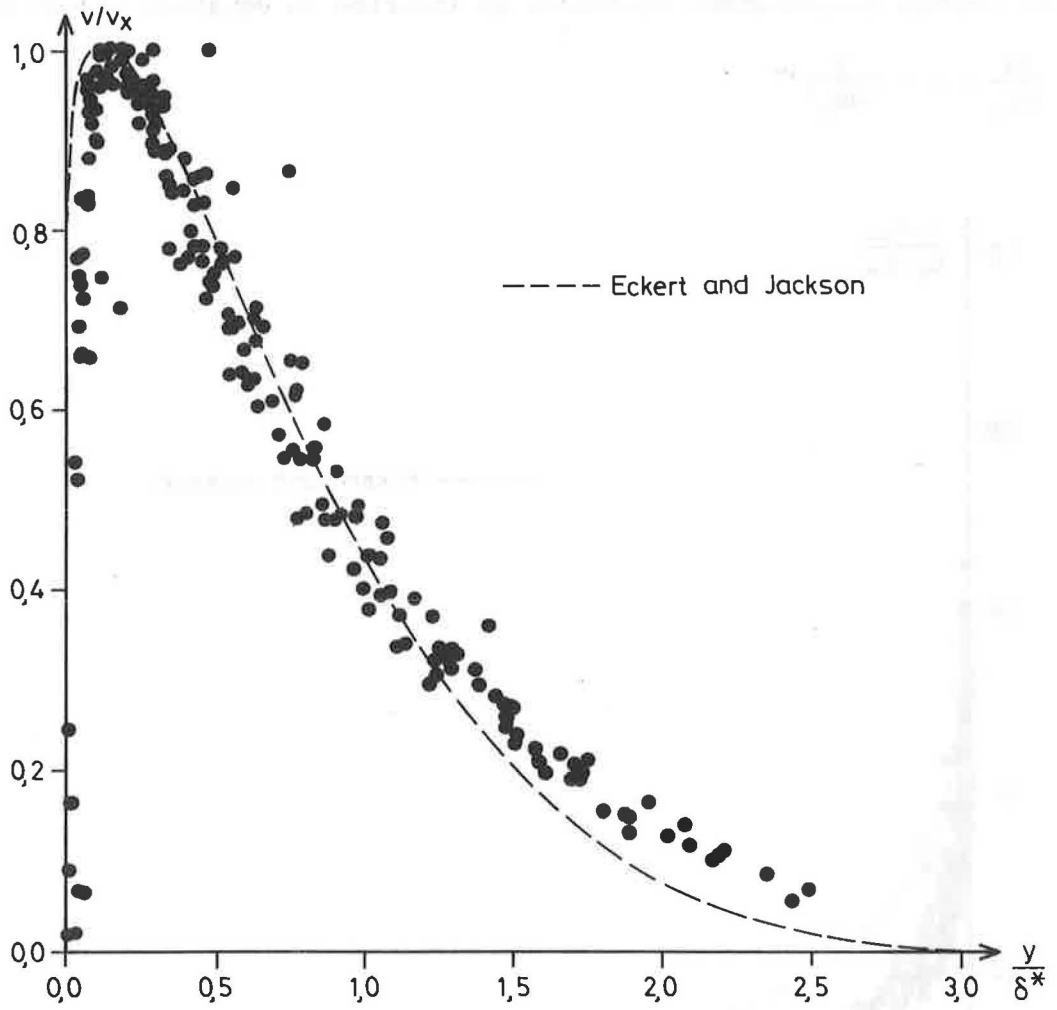

Figure 6. Recorded velocity distribution in the boundary layer.

The assumed shapes for temperature and velocity profiles, equations (24) and (26), respectively, in the boundary layer flow do not fit well with the recorded profiles. Measurements in turbulent boundary layers by Cheesewright, [6] and [7], Vliet and Liu, [8], and Warner and Arpaci, [9], have shown the same disagreement.

The measured values of the maximum velocity, the boundary layer thickness and the volumetric flow rate are compared with both the wall and the cylinder solution. The results are shown in the figures 7, 8 and 9, respectively.

The numerical solution shows that the curvature of the cylinder does not affect the magnitude of the maximum velocity to any great extent. The recorded maximum velocities in figure 7 are only half of the predicted velocities.

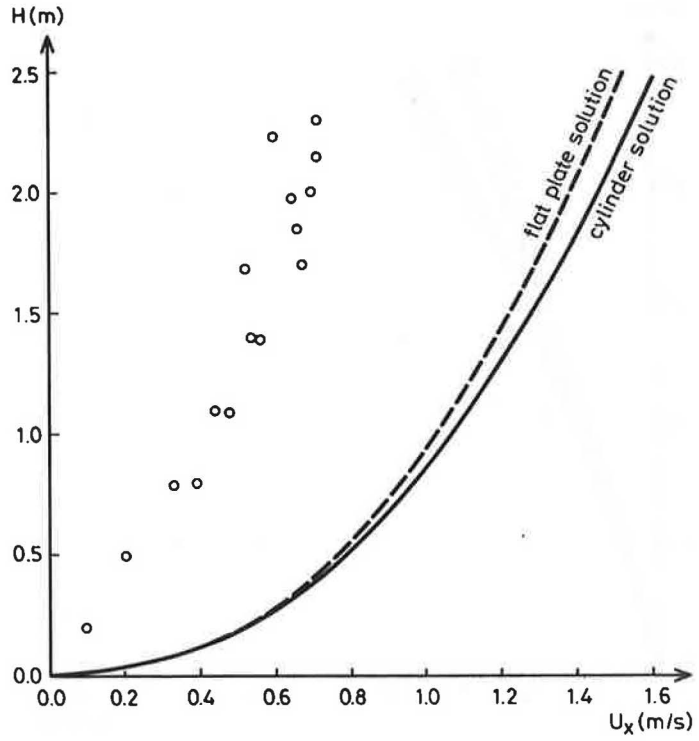

Figure 7. Maximum velocities in the turbulent natural convection boundary layer flow. Recorded and calculated in the flat plate and the cylinder case at constant heat flux from the surface q" = 680 W/m^2.

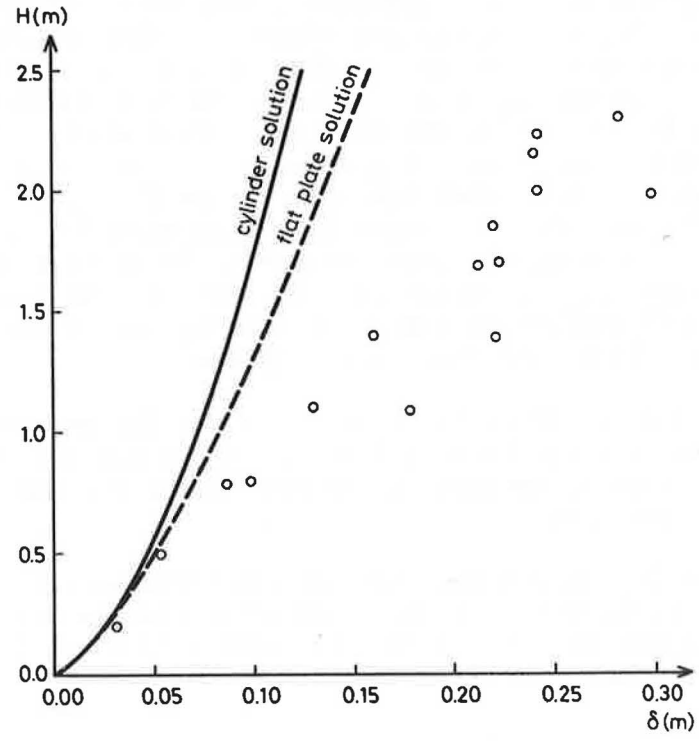

Figure 8. Boundary layer thickness in the turbulent natural convection boundary layer flow. Recorded and calculated in the flat plate and the cylinder case at constant heat flux from the surface q" = 680 W/m^2.

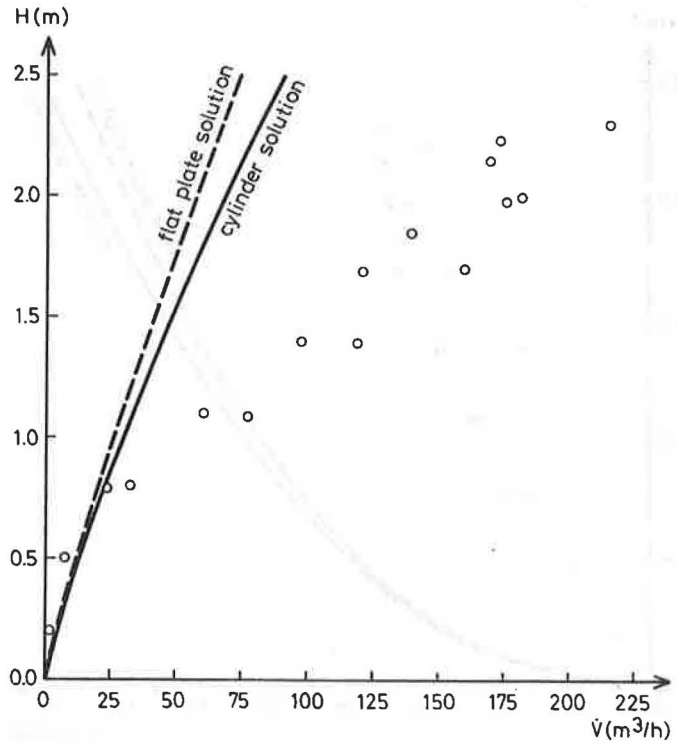

Figure 9. Volume flow in the turbulent natural convection boundary layer flow. Recorded and calculated in the flat plate and the cylinder case at constant heat flux from the surface $q'' = 680\ W/m^2$.

The result in figure 8 shows the opposite trend. Here the recorded boundary layer thickness is larger than the predicted one. The results in figure 7 and 8 with lower maximum velocities and thicker boundary layer than predicted from the profiles suggested by Eckert and Jackson are in accordance with the measurements reported by Kriegel, [5]. The volumetric flow rate in the boundary layer flow is calculated by numerical integration of the recorded velocity profiles. The result in figure 9 shows that the theoretical flow rate is much smaller than the recorded flow rate. The convective flow around a cylindrical surface entrains a larger amount of air from the surroundings than the convective flow along a flat plate. The volumetric flow rate in the boundary layer flow around a cylindrical surface is therefore growing faster and becomes larger than the volumetric flow rate along a flat plate.

The predictions from the theoretical analysis and the measurements in the boundary layer flow are far from each other. It is possible to get a better prediction of the flow parameters, if better shapes for the velocity and temperature profiles are used.

In the analysis it is implied that the ambient temperature is a constant. The measurements were performed in a test room with displacement ventilation and a temperature gradient of 1 - 2 $^{o}C/m$. This will influence the boundary layer flow around the cylinder.

TEMPERATURE IN THE ROOM

The distribution of room air temperature is shown in figure 10. The power supplied to the cylinder amounted to 600 watt. The room air temperature is given in non-dimensional form as the difference between the temperature in

the room and the temperature in the supply, $(T-T_s)$, divided by the difference between the temperature in the extract and in the supply, (T_e-T_s). The temperature gradient varied between 1.2°C/m to 3.1°C/m.

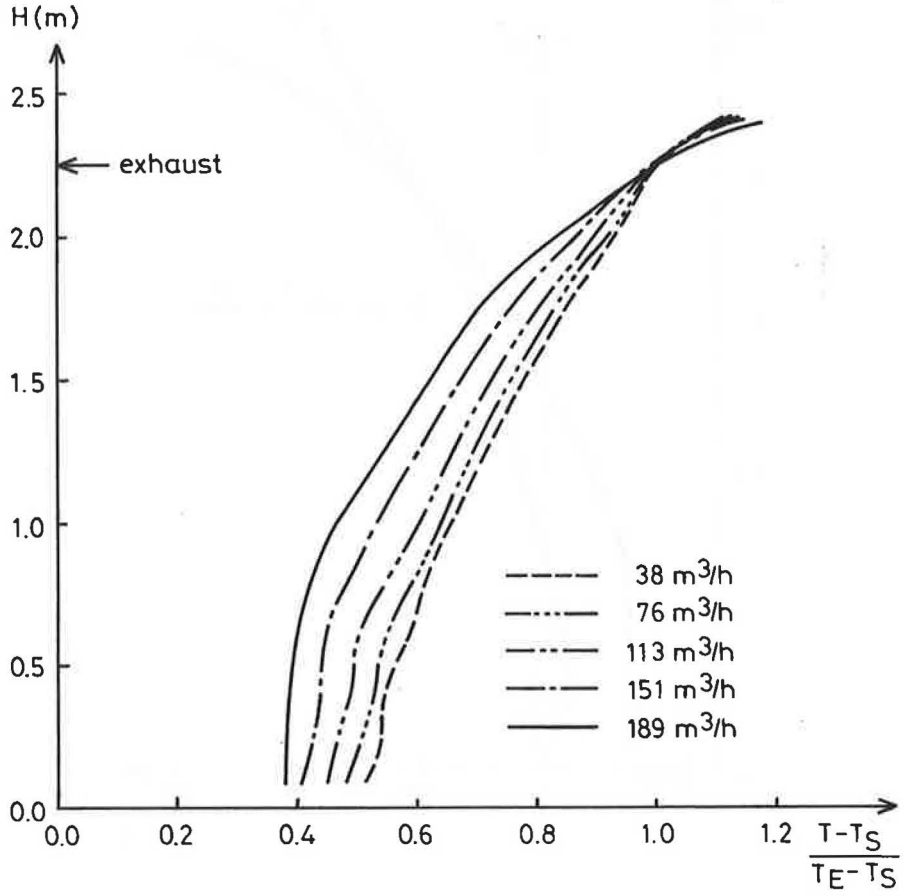

Figure 10. Prescribed temperature distribution in the room. Heat load 600 W, specific air flow rates n = 1 - 5 roomv./h.

At floor level the temperature difference between the room air and the extract is about half of the temperature difference between the extract and the supply. Measurements of the floor temperature and the room air temperature close to the floor show that the floor surface is warmer than the air layer above the floor. The relatively high floor temperature is an effect of heat transferred to the floor by radiation from the ambient surfaces. Calculation of the radiation heat transfer based on recorded surface temperature shows that 20% of the total power supply is radiated from the ceiling to the floor. To this is added the radiation from the walls to the floor. Therefore, a large fraction of the total heat supply is redistributed by long wave thermal radiation to the lower part of the room. This radiation heat transfer will diminish the temperature difference between the upper - and the lower part of the room.

Room air temperature and surface temperature of the walls are shown in figure 11 for one combination of power supplied to the cylinder and specific air flow rate. The wall temperature presented is the average of all four walls. The level of stratification found by smoke visualization and the temperature of the surroundings are also shown.

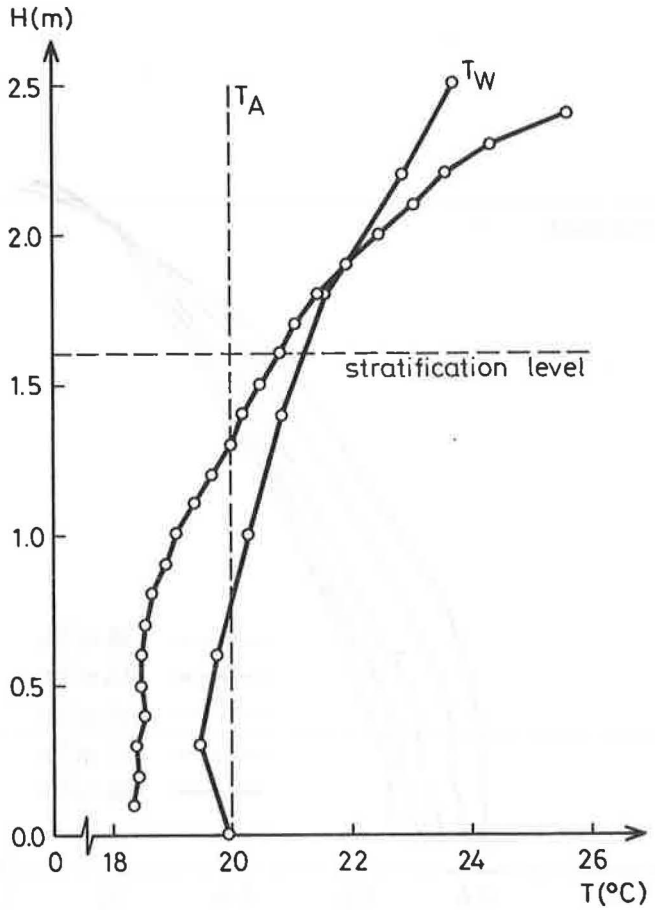

Figure 11. Room air and wall surface temperatures in the room at a heat load of 600 W and a specific flow rate of n = 5 roomv./h.

In the lower part of the room the wall surface temperature is higher than the room air temperature, while it is the opposite in the upper part. There will be a free convective flow along the walls from the lower part to the upper part of the room.

The average temperature outside the test room is about 20°C. In the lower part of the room there will therefore be an inflow of heat through the walls from the surroundings, while there will be a transmission loss of heat in the upper part.

With this heat source the recorded room air temperature profiles do not reveal anything about the stratified flow that occurs in the room. This is due to the circumstance that the temperature field in the room is not only affected by the air flow pattern. Redistribution of heat due to radiation heat transfer and heat transfer at walls will also influence the room air temperature.

STRATIFICATION IN THE ROOM

The idea behind ventilation by displacement is to achieve supply air conditions in the occupied zone. Therefore, the level of stratification at dif-

ferent ventilation air flow rates is of vital importance for a designer of ventilation systems. In the previous subsection it was shown that the vertical temperature profiles were modified by the redistribution of heat due to radiation, transfer of heat through the building envelope and convective flows along the walls. Therefore, they did not reveal any information about the stratification in the room. In order to gain insight in the stratification in the room tracer gas was released into the room.

In figure 12 the stationary distribution of contaminants is shown with release of tracer gas into the boundary layer flow around the cylinder. The recorded concentrations are given in relation to the maximum recorded concentration. The power supplied to the cylinder amounted to 600 watt.

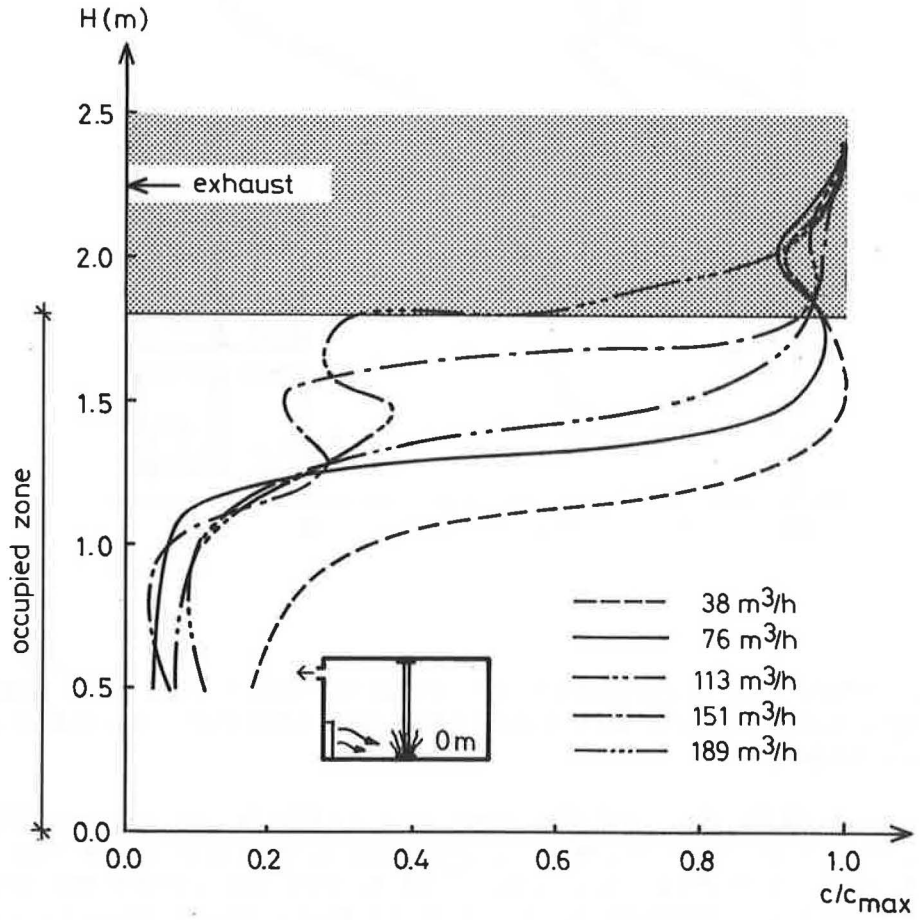

Figure 12. Prescribed distribution of contaminants in the room with release of tracer gas into the boundary layer flow.

Figure 12 shows clearly the levels of stratification in the room. Here the boundary layer flow around the cylinder is the only source. The level of stratification rises when the air flow rate is increased, and a large air flow rate is required to move the level of stratification above the occupied zone.

The distribution of contamination in figure 12 is found in a situation where the heat and the contaminant source were the same. In figure 13 the distribution of contamination is shown in two situations where the release of tracer gas is moved from the boundary layer flow to the ambient, above and below the level of stratification, respectively.

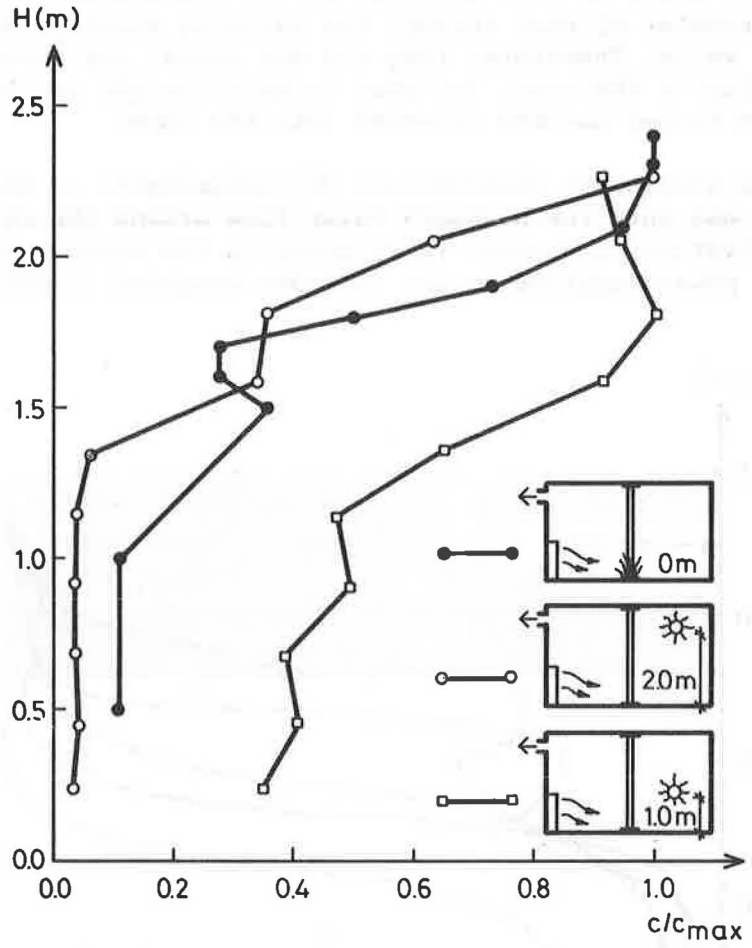

Figure 13. Prescribed distribution of contamination in the room with release of tracer gas into the boundary layer flow and into the room 2.0 m and 1.0 m above floor, respectively.

The power supplied to the cylinder amounted to 600 W and the specific air flow rate was n = 5 roomv./h. With release of tracer gas above the level of stratification only a very small amount of tracer gas enters the lower zone, and the concentration becomes only 3 - 4% of the maximum recorded concentration. With release of tracer gas below the level of stratification, some of the tracer gas is spread in the lower zone before it is slowly evacuated from the room. The concentrations in the lower zone become about half of the concentration in the upper zone.

In principle the volume flow around the cylinder could be decided on the basis of the levels of stratification in the room. As it can be seen from figure 12, it is only possible to get a rough estimate of the level of stratification from the distribution of contaminants. In figure 14 the level of stratification is compared with the measured volume flows around the cylinder. The level of stratification is defined as the height above the floor where the concentration is half of the maximum recorded concentration.

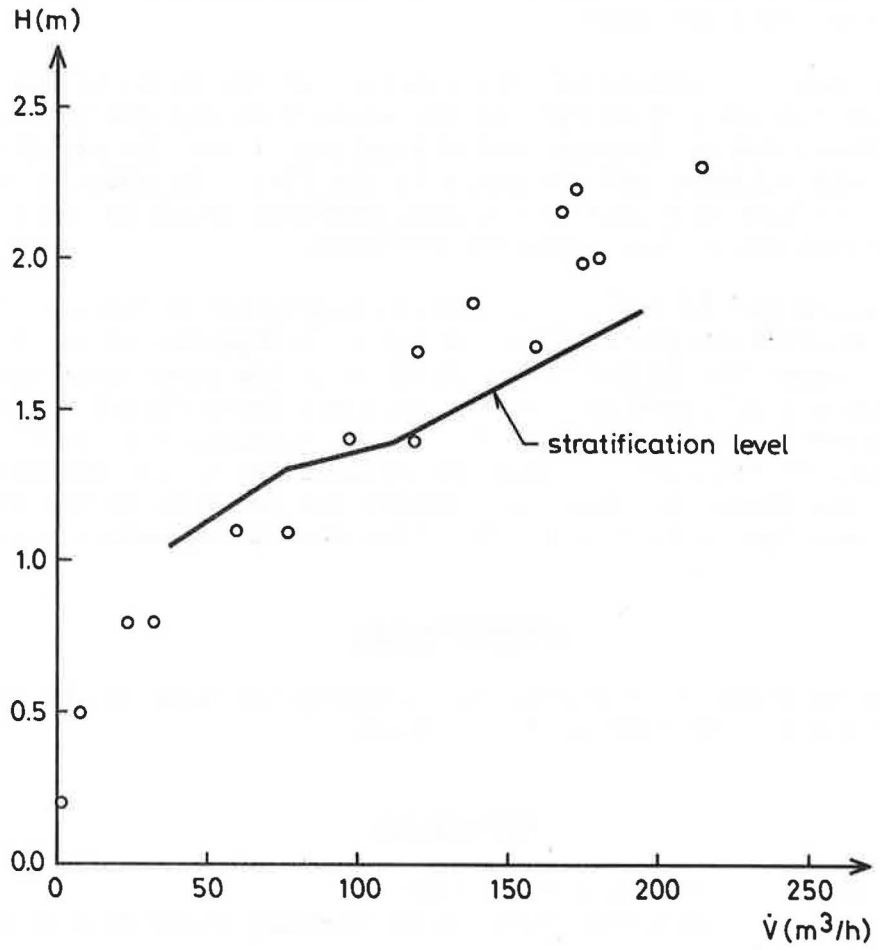

Figure 14. Measured volume flow around the cylinder compared with the level of stratification.

Figure 14 shows a reasonable correspondence between measured volume flow and the level of stratification. Especially if the influence of the convective flow at the walls is taken into consideration.

CONCLUSION

The analysis of turbulent natural convection boundary layers made by Eckert and Jackson has been slightly generalized by studying natural convection along a vertical slender cylinder. The wall case will then be the special case where the thickness of the boundary layer flow is much less than the radius of the cylinder. The analysis has been extended to include the case with constant heat flux from the surface.

The solutions for wall and cylinder surfaces are given for both the constant temperature case and the constant heat flux case as simplified, ease to use relations.

Comparison with measurements in the boundary layer along a slender cylinder in a ventilated room showed that the predicted values did not fit very well. The predicted value for maximum velocity was twice the measured value, while

the predicted values for boundary layer thickness and volume flow were considerably lower than the measurements. It is probably possible to get an improved prediction if better shapes for the temperature and velocity profiles in the boundary layer are used.

It was found that the temperature distribution in the room did not reveal anything about the stratified flow in the room. This was due to the circumstance that there was an internal redistribution of heat by radiation from the ceiling, the cylinder and the walls to the floor. In addition there was heat transfer through the surrounding room surfaces (both in and out), which caused a boundary layer flow along the surfaces.

Release of tracer gas into the room showed clearly the stratified flow in the room. The concentration distribution in the room depended on the location of tracer gas release. The highest concentration in the lower zone occured when the tracer gas was released outside the boundary layer flow 1 m above the floor. The concentration was then half of the concentration in the upper zone. It was possible to estimate the level of stratification for different volumetric air flow rates. A comparison between the measured volume flow around the cylinder and the level of stratification showed reasonable correspondence.

ACKNOWLEDGMENT

We would like to thank C. Blomqvist for carrying out some of the tracer gas measurements and for the technical assistance.

REFERENCES

[1] Eckert, E.R.G., Jackson, T.W. (1951),
Analysis of Turbulent Free-Convection Boundary Layer on Flat Plate,
NACA Report 1015.

[2] Bayley, F.J. (1955),
An Analysis of Turbulent Free-Convection Heat Transfer,
Proc. of the Instn. of Mech. Engrs., Vol. 169, No. 20, pp 361-368.

[3] George, W.K., Capp, S.P. (1979),
A Theory for Natural Convection Turbulent Boundary Layers next to Heated Vertical Surfaces,
Int. J. Heat Mass Transfer, Vol. 22, pp 813-826.

[4] Griffiths, E. Davis, A.H. (1922),
The Transmission of heat by Radiation and Convection,
Special report No. 9, British Food Investigation Board.

[5] Kriegel, B. (1973),
Kalluftabfall an Abkühlungsflächen,
Klima-Kälte-technik No. 4.

[6] Cheesewright, R. (1968),
Turbulent Natural Convection from a Vertical Plane Surface,
Journal of Heat Transfer. Trans. Asme. Series C., Vol. 90, No. 1, pp 1-8.

[7] Cheesewright, R., Ierokiopitis, E. (1982),
Velocity Measurements in a Turbulent Natural Convection Boundary Layer,
Int. Heat Transfer conf., München, Vol. 2, pp 305-309.

[8] Vliet, G.C., Liu, C.K. (1969),
An Experimental Study of Turbulent Natural Convection Boundary Layers,
Journal of Heat Transfer, Vol. 91, pp 517-531.

[9] Warner, C.Y., Arpaci, V.S. (1968),
An Experimental Investigation of Turbulent Natural Convection in Air at Low Pressure along a Vertical Heated Flat Plate,
Int. J. Heat Transfer, Vol. 11, pp 397-406.